

Ensemble averaged Madelung energies of finite volumes and surfaces

Peter Krüger
Graduate School of Engineering and
Molecular Chirality Research Center,
Chiba University, Chiba 263-8522, Japan
pkruger@chiba-u.jp

May 22, 2020

Abstract

Exact expressions for ensemble averaged Madelung energies of finite volumes are derived. The extrapolation to the thermodynamic limit converges unconditionally and can be used as a parameter-free real-space summation method of Madelung constants. In the large volume limit, the surface term of the ensemble averaged Madelung energy has a universal form, independent of the crystal structure. The scaling of the Madelung energy with system size provides a simple explanation for the structural phase transition observed in cesium halide clusters.

1 Introduction

The cohesive energy of ionic crystals is dominated by the electrostatic energy between ionic point charges, known as the Madelung energy. The calculation of Madelung energies is a mathematically non-trivial problem because of the long-range nature of the Coulomb interaction. The Madelung constant of basic crystal structures was first successfully calculated by Ewald [1]. In the Ewald method, the Coulomb interaction is divided into a short range part for which the Madelung sum converges fast in real space and a long range part which can be summed in reciprocal space. The Ewald method is very accurate and widely used, but it is numerically rather involved and relies on periodic boundary conditions. Alternatively, the Madelung energy can be calculated through direct summation in real space, which is numerically simpler and can be used in finite system [2] and non-periodic structures.

However, the lattice sums are only conditionally convergent, i.e. the result depends on the summation order. This reflects the physical fact that in a finite crystal, the potential at an inner site can be changed at will by choosing particular surface terminations [3]. In three dimensions, the Madelung sums diverge for the most natural, shell-like summation order [4]. Divergence can be avoided in two ways. In the first type of methods, the lattice is divided into neutral cells of vanishing dipole moment [5]. The sum over these cells converges absolutely because the quadrupole-quadrupole interaction decays as $1/r^5$. However, dipole moment free cells generally involve fractional ions at the corners and edges, and can be difficult to construct for low symmetry systems [6]. In the second type of method, the summation is done in the natural order of increasing distance but the system is neutralized at each step by adding a background or surrounding sphere [7, 8]. An example is the Wolf method [7] which keeps only the short-range part of the Ewald method but compensates each charge inside the summation sphere by an opposite charge at the cut-off radius.

Here we consider ensemble averaged quantities in finite subvolumes of a macroscopic system, especially the mean electrostatic potential at the sites of a given ionic species. This leads to an alternative definition of Madelung energies which converges unconditionally as a function of system size for any subvolume shape. We derive an exact expression of the Madelung constants in finite spheres. The leading term in the expansion over inverse size is found to be independent of the crystal structure. As a consequence, the Madelung contribution to the surface energy, averaged over surface orientations, is the same for all crystal structures, and provides a universal first order approximation of the surface energy of ionic systems. We apply the theory to the relative stability of CsCl and NaCl ionic structures as a function of system size. Under the assumption of equal nearest neighbor distance we find that the stable structure switches from NaCl to CsCl when the system size exceeds a few hundred ions, which explains the phase transition observed in cesium halide clusters.

2 Average Madelung energy of finite volumes

We consider a collection of N point charges at positions \mathbf{r}_i^α , where α labels the different species with charge q_α . The electrostatic energy is given by

$$U = \frac{1}{2} \sum_{j\beta \neq i\alpha} \frac{q_\alpha q_\beta}{|\mathbf{r}_i^\alpha - \mathbf{r}_j^\beta|} = \frac{1}{2} \sum_\alpha q_\alpha \sum_i \phi(\mathbf{r}_i^\alpha) \quad (1)$$

where

$$\phi(\mathbf{r}_i^\alpha) = \sum_{j\beta(\neq i\alpha)} \frac{q_\beta}{|\mathbf{r}_i^\alpha - \mathbf{r}_j^\beta|}. \quad (2)$$

is the electrostatic potential at site \mathbf{r}_i^α . For crystals we take each ion in the unit cell as a different species α and i is the cell index. In the infinite crystal, $\phi(\mathbf{r}_i^\alpha)$ is independent of i . The Madelung constant of the species α is commonly defined as

$$M_\alpha = -\phi(\mathbf{r}_i^\alpha)d/q_\alpha, \quad (3)$$

where d is the nearest neighbor distance. In a practical real space summation, one computes the potential $\phi(\mathbf{r}_i^\alpha)$ at some site i of a finite cluster (usually the central site), and lets the cluster size N go to infinity. The problem with this approach is that the series in Eq. (2), converges only conditionally for $N \rightarrow \infty$. This means that the sum, i.e. the potential at site i , depends on the summation order and may diverge.

Instead of the potential at a given site i , we consider the average potential at the sites of the α -ions,

$$\bar{\phi}_\alpha = \frac{1}{N_\alpha} \sum_{ij\beta}^{i \neq j} \frac{q_\beta}{|\mathbf{r}_i^\alpha - \mathbf{r}_j^\beta|} \quad (4)$$

where N_α is the number of α ions in the cluster. The electrostatic energy in Eq. (1) can be rewritten as

$$U = \frac{1}{2} \sum_\alpha N_\alpha q_\alpha \bar{\phi}_\alpha. \quad (5)$$

Equations (1) and (5) are equivalent and hold for finite and infinite systems. For an infinite crystal, we obviously have $\bar{\phi}_\alpha = \phi(\mathbf{r}_i^\alpha)$. This suggests a redefinition of the Madelung constants as

$$M_\alpha = -\bar{\phi}_\alpha d/q_\alpha. \quad (6)$$

Of course, as with Eqs. (2,3), the true Madelung constants are obtained in the limit $N \rightarrow \infty$. The advantage of definition (6) is that the electrostatic energy can be expressed simply in terms of M_α as

$$U = -\frac{1}{2d} \sum_\alpha N_\alpha M_\alpha q_\alpha^2, \quad (7)$$

which holds for any system, finite or infinite.

We introduce the particle density of species α

$$\rho_\alpha(\mathbf{r}) = \left\langle \sum_i \delta(\mathbf{r} - \mathbf{r}_i^\alpha) \right\rangle \quad (8)$$

where $\langle \dots \rangle$ denotes a statistical ensemble average. The pair distribution function is defined as

$$g_{\alpha\beta}(\mathbf{r}, \mathbf{r}') = \frac{1}{\rho_\alpha(\mathbf{r})\rho_\beta(\mathbf{r}')} \left\langle \sum_{ij}^{i \neq j} \delta(\mathbf{r} - \mathbf{r}_i^\alpha) \delta(\mathbf{r}' - \mathbf{r}_j^\beta) \right\rangle. \quad (9)$$

With these functions, we can rewrite the ensemble average of the Eq. (4), as

$$\langle \bar{\phi}_\alpha \rangle = \frac{1}{N_\alpha} \sum_\beta q_\beta \int d\mathbf{r} \rho_\alpha(\mathbf{r}) \int d\mathbf{r}' \rho_\beta(\mathbf{r}') \frac{g_{\alpha\beta}(\mathbf{r}, \mathbf{r}')}{|\mathbf{r} - \mathbf{r}'|}. \quad (10)$$

Now we consider a finite subvolume V of an infinite ionic solid and average over all possible positions and orientations of V . Equivalently we can keep the subvolume fixed in space and perform statistical averaging in an ensemble of crystals of random position and orientation, which is realized in a powder sample. This ensemble is homogeneous and isotropic, i.e. it has the symmetry of a fluid, where the density ρ_α is a constant, and the pair distribution function $g_{\alpha\beta}(r)$ depends only on the distance $r = |\mathbf{r}_i^\alpha - \mathbf{r}_j^\beta|$ [9]. As a result, and using $\rho_\alpha = N_\alpha/V$, Eq. (10) simplifies to

$$\langle \bar{\phi}_\alpha \rangle = \frac{1}{V} \sum_\beta \rho_\beta q_\beta \int_V d\mathbf{r} \int_V d\mathbf{r}' \frac{g_{\alpha\beta}(|\mathbf{r} - \mathbf{r}'|)}{|\mathbf{r} - \mathbf{r}'|}. \quad (11)$$

This expression holds for a finite subvolume V of any homogeneous and isotropic ensemble, in particular for a fluid or powder sample. Further, as explained above, statistical averaging in such an ensemble is equivalent to considering a single crystal and averaging over the position and orientation of the subvolume V . Hence Eq. (11) also holds in this sense. In standard direct space lattice summation methods, a finite cluster size corresponds to a subvolume of the infinite crystal with fixed center and orientation as illustrated in Fig. 1 (a). In the present method, an average is done over all possible positions and orientations (Fig. 1 b). In the special case of a spherical subvolume considered in the numerical applications below, only positional averaging is meaningful. However, the main results and conclusions are independent of the subvolume shape.

For stability, any ionic system must be *globally* charge neutral, i.e.

$$\sum_\alpha \rho_\alpha q_\alpha = 0. \quad (12)$$

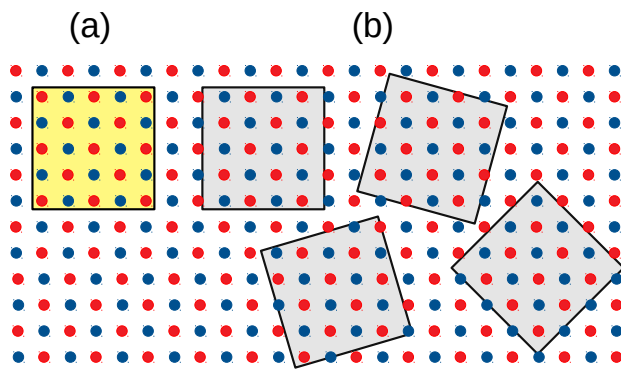


Figure 1: Illustration of the difference between a standard real-space summation method (a), and the present, ensemble averaged method (b). Red and blue dots are positive and negative point charges and the black lines indicate the boundary of the finite cluster volume V . In (a) the center and orientation of the volume V is fixed. In (b) an average is done over all possible positions and orientations of V .

We do not assume any form of *local* charge neutrality. Averaging is done over all configurations in the ensemble, including those where the finite volume V has a net charge. By virtue of Eq. (12), we may add to the integrand in Eq. (11) any function $f(\mathbf{r}, \mathbf{r}')$ that is independent of α , without changing the value of the expression. We shall add $-1/|\mathbf{r} - \mathbf{r}'|$, i.e. we replace $g_{\alpha\beta}(r)$ by the pair correlation function $h_{\alpha\beta}(r) \equiv g_{\alpha\beta}(r) - 1$ and obtain

$$\langle \bar{\phi}_\alpha \rangle = \sum_\beta \rho_\beta q_\beta H_{\alpha\beta}^V, \quad (13)$$

where

$$H_{\alpha\beta}^V = \frac{1}{V} \int_V d\mathbf{r} \int_V d\mathbf{r}' h_{\alpha\beta}(|\mathbf{r} - \mathbf{r}'|) v(|\mathbf{r} - \mathbf{r}'|) \quad (14)$$

with $v(r) = 1/r$. For $V \rightarrow \infty$, this simplifies to

$$H_{\alpha\beta}^\infty = \int_0^\infty h_{\alpha\beta}(r) v(r) 4\pi r^2 dr. \quad (15)$$

While we focus on the bare Coulomb potential $v(r) = 1/r$, the present theory can in principle be applied to any potential form $v(r)$. For the special case $v = 1$, $H_{\alpha\beta}^\infty$ are the Kirkwood-Buff integrals (KBI, usually denoted G rather than H) of solution theory [10]. Previously we have extended KBI theory to finite volumes [11]. We showed that the bad convergence of the usual, truncated integrals can be avoided by an exact transformation from double volume integrals to one-dimensional radial integrals. Using this formalism [12, 13], we rewrite Eq. (14) as

$$H_{\alpha\beta}^V = \int_0^\infty h_{\alpha\beta}(r) v(r) w^V(r) dr \quad (16)$$

where

$$w^V(r) = \frac{1}{V} \int_V d\mathbf{r}_1 \int_V d\mathbf{r}_2 \delta(r - |\mathbf{r}_1 - \mathbf{r}_2|) \quad (17)$$

is a weight function. Note that Eq. (16) is actually a finite integral, since $w^V(r) = 0$ for $r > L_{\max}$ where L_{\max} is the maximum distance in V . Equations (6,13,16,17) provide an exact expression for the ensemble averaged Madelung potential in finite volumes. The weight function is conveniently expressed as

$$w^V(r) = 4\pi r^2 y(r/L) \quad (18)$$

where $L = 6V/A$ and A is the surface area. The function $y(x)$ only depends on the shape of the volume [13]. For a sphere of diameter L , the exact expression is [11]

$$y_s(x) = (1 - 3x/2 + x^3/2)\theta(1 - x) \quad (19)$$

where $\theta(x)$ is the unit step function ($\theta=0$ for $x<0$ and $\theta=1$ for $x>0$). Analytic expressions of $y(r)$ are also known for cube and cuboid [13]. For any other shape, the function can be easily computed numerically [14]. In order to accelerate convergence to the thermodynamic limit, several extrapolations from the finite volume integrals have been proposed [11, 13, 15]. Here we focus on the second order expression of Ref. [13], with weight function $u_2(r) = 4\pi r^2 y_2(r/L)$, where

$$y_2(x) = (1 - 23x^3/8 + 3x^4/4 + 9x^5/8)\theta(1 - x) \quad (20)$$

For further reference, we also define

$$y_0(x) = \theta(1 - x) \quad (21)$$

which corresponds to simple truncation of radial integrals or lattice sums at $r = L$.

3 Application to crystals

In the following, we consider a crystal with unit cell of volume V_c containing m point charges q_α , $\alpha = 1 \dots m$, at positions \mathbf{r}^α . We take each atom in the unit cell as a different species α , such that $\rho_\alpha = 1/V_c$ for all α . The spherically averaged pair distribution function, appropriate for powder samples, is given by

$$g_{\alpha\beta}(r) = \frac{V_c}{4\pi r^2} \sum'_{\mathbf{T}} \delta(r - |\mathbf{r}^\alpha - \mathbf{r}^\beta + \mathbf{T}|), \quad (22)$$

where \mathbf{T} are lattice vectors and the primed sum indicates that the term $\mathbf{T} = 0$ is excluded for $\alpha = \beta$. Equivalently, Eq. (22) may be written as a sum over shells,

$$g_{\alpha\beta}(r) = \frac{V_c}{4\pi r^2} \sum_k n_k^{\alpha\beta} \delta(r - R_k^{\alpha\beta}) \quad (23)$$

where $n_k^{\alpha\beta}$ is the number of β ions on shell number k of radius $R_k^{\alpha\beta} = |\mathbf{r}^\alpha - \mathbf{r}^\beta + \mathbf{T}| > 0$ around an α ion. Inserting Eq. (23) into Eq. (16) we obtain

$$H_{\alpha\beta}^V = V_c \sum_k n_k^{\alpha\beta} v(R_k^{\alpha\beta}) y(R_k^{\alpha\beta}/L) - B^V \quad (24)$$

where

$$B^V = \int_0^\infty v(r) y(r/L) 4\pi r^2 dr. \quad (25)$$

The term B^V comes from the constant 1 which was subtracted when going from $g_{\alpha\beta}$ to $h_{\alpha\beta}$ in Eqs (11,13). By virtue of Eq. (12) the B^V terms cancel upon summing over β in Eq. (13). While B^V has no direct physical meaning, it is important for the convergence of the individual terms $H_{\alpha\beta}$ in Eq. (24). For a sphere of diameter L , we obtain $B^V = 4\pi L^3 \int_0^1 v(xL)y_s(x)x^2 dx$ with y_s given in Eq. (19). For the Coulomb interaction, $v(r) = 1/r$, this yields $B^V = 2\pi L^2/5 = (12/5)V/L$. For $v = 1$ (KBI) we have $B^V = \pi L^3/6 = V$.

In the following we consider a sphere of diameter L and calculate, with $y = y_s$ (Eq. 19), the exact finite volume integrals $H_{\alpha\beta}^V$ (Eq. 24) and the corresponding ensemble averaged Madelung constants (Eqs 6,13). We also compute extrapolations of $H_{\alpha\beta}^V$ to infinite volume, obtained with $y = y_2$ (Eq. 20) as well as the usual, unweighed sums truncated at $r = L$, obtained with $y = y_0$ (Eq. 21). The convergence of the Madelung constant of the NaCl structure is shown in Fig. 2. The exact, infinite lattice value is $M^\infty = 1.7475646$. The relative error $|M(L)/M^\infty - 1|$ is plotted as a function of system size L . The exact finite volume result (y_s) converges very smoothly as $1/L$ while the y_2 -extrapolation (y_2) converges as $1/L^2$. The truncated sum with $y = y_0$ corresponds to the most simple summation order over spherical shells. As it is well known, this summation order strongly diverges for the NaCl structure [4] and the result is not shown in Fig. 2.

We have examined the effect of charge neutralization using the shifted potential method by Wolf *et al.* [7], which consists in replacing the true Coulomb interaction $q_i q_j / r_{ij}$ by $q_i q_j (1/r_{ij} - 1/L)$. For the usual, truncated sum (y_0), this is equivalent to adding a term $-Q/L$ to the potential, where Q is the total charge in the sphere of radius L [7, 8]. Charge neutralization makes the truncated sum converge, roughly as $1/L$, as seen from the curve y_0 -N in Fig. 2. Interestingly, for the exact finite volume integrals (y_s), charge neutralization has almost no effect. Indeed, the curve with charge neutralization (y_s -N) is almost identical to that without (y_s). This indicates that the positional averaging (see Fig. 1), which is implicit in y_s , largely cancels charge imbalances and makes explicit charge neutralization unnecessary. For the y_2 extrapolation, however, charge neutralization speeds up convergence considerably and the charge-neutralized sums (y_2 -N) converge as $1/L^3$, in the same way as y_2 -extrapolated, proper KBI integrals [13]. For comparison, the Wolf method [7] is also shown with an Ewald damping parameter $\alpha = 0.5$. Because of the $\text{erfc}(\alpha r)$ -like damping term used in this scheme, the lattice sum converges exponentially fast and thus outperforms any method with power-law convergence, such as the present one. However, the Wolf method requires an empirical parameter (α), whose optimum

value depends on the problem at hand. As seen from Fig. 2, with the present scheme y_2 -N, a practically reasonable error of 10^{-3} is achieved with a very moderate cut-off $L = 10d$, which is comparable to $L = 6d$ needed with the Wolf method. In conclusion of this section we have shown that ensemble averaged Madelung constants, Eqs (6,11), converge unconditionally even without charge compensation or damping factors. The y_2 -extrapolation with charge neutralization converges as $1/L^3$, which is quite fast, albeit slower than the Wolf method.

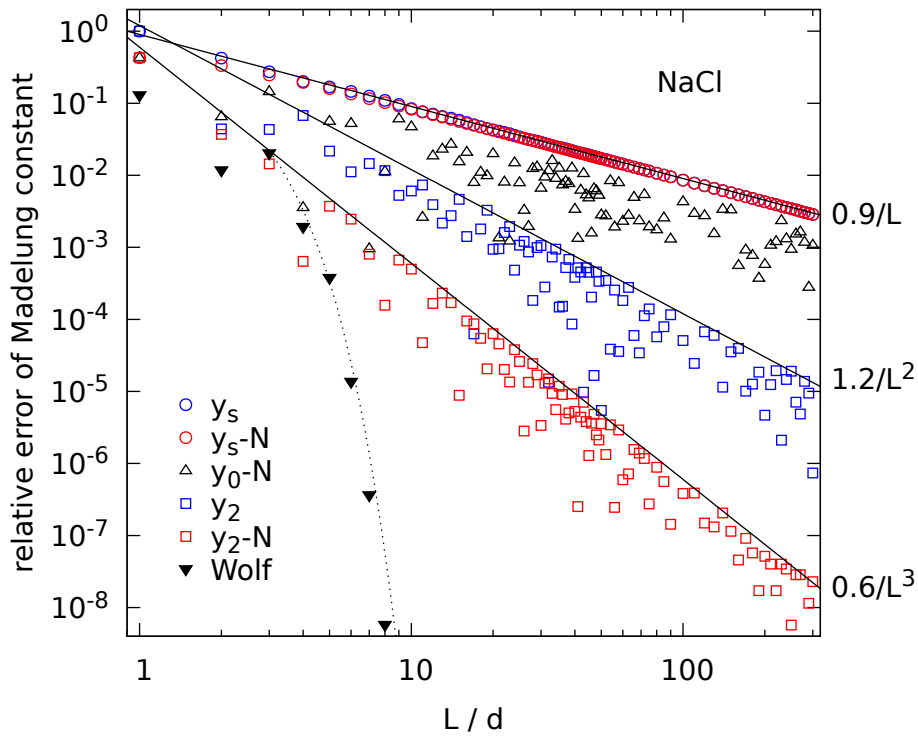


Figure 2: Relative error $|M(L)/M^\infty - 1|$ of the Madelung constant of NaCl computed as function of sphere diameter L . Finite volume result (y_s , blue circles), y_2 -extrapolation (blue squares) and the same with charge neutralization (y_s -N and y_2 -N, red symbols), truncated sum with charge neutralization (y_0 -N, up triangles) and the Wolf method [7] with damping parameter $\alpha = 0.5$ (filled down triangles) are compared. The solid lines are power law fits of the maximum error and the dotted line is a guide to the eye.

4 Size dependence of Madelung energies

4.1 Universal surface term

Finite volume integrals like H^V in Eq. (16) can be expanded in powers of $1/L$ as [13]

$$H_{\alpha\beta}(L) = H_{\alpha\beta}^{\infty} + F_{\alpha\beta}^{\infty}/L + \mathcal{O}(L^{-2}), \quad (26)$$

where $F_{\alpha\beta}^{\infty}$ is the surface term in the large volume limit, given by

$$F_{\alpha\beta}^{\infty} = -\frac{3}{2} \int_0^{\infty} r h_{\alpha\beta}(r) v(r) 4\pi r^2 dr. \quad (27)$$

For the Coulomb potential $v(r) = 1/r$, this simplifies to $F_{\alpha\beta}^{\infty} = -3G_{\alpha\beta}^{\infty}/2$, where

$$G_{\alpha\beta}^{\infty} = \int_0^{\infty} h_{\alpha\beta}(r) 4\pi r^2 dr \quad (28)$$

is a proper KBI. The latter is directly related to the particle number fluctuations in the volume V as [16]

$$\rho_{\alpha} G_{\alpha\beta}^{\infty} = \frac{\langle N_{\alpha} N_{\beta} \rangle - \langle N_{\alpha} \rangle \langle N_{\beta} \rangle}{\langle N_{\beta} \rangle} - \delta_{\alpha\beta}. \quad (29)$$

Here we are interested in a solid at low temperature where the fluctuations are negligible, i.e. $\rho_{\alpha} G_{\alpha\beta}^{\infty} = -\delta_{\alpha\beta}$ and so

$$F_{\alpha\beta}^{\infty} = (3/2)\delta_{\alpha\beta}/\rho_{\alpha}. \quad (30)$$

Using Eqs. (13,26,30), the size dependence of the ensemble averaged Madelung constants (6) is found to be

$$M_{\alpha}(L) = M_{\alpha}^{\infty} - (3/2)d/L + \mathcal{O}(L^{-2}), \quad (31)$$

which holds for all ionic species and *for any structure*. This is exemplified with a few crystal structures types in Fig. 3. It can be seen that all Madelung constants approach the infinite volume limit with the same slope $-3/2$, confirming the general validity of Eq. (31).

From Eqs (7,31) and $L = 6V/A$, the surface contribution to the Madelung energy, per area A , is given by

$$U^S = \rho \langle q^2 \rangle / 8, \quad (32)$$

where $\rho = \sum_{\alpha} \rho_{\alpha}$ is the total particle density and

$$\langle q^2 \rangle = \sum_{\alpha} N_{\alpha} q_{\alpha}^2 / N \quad (33)$$

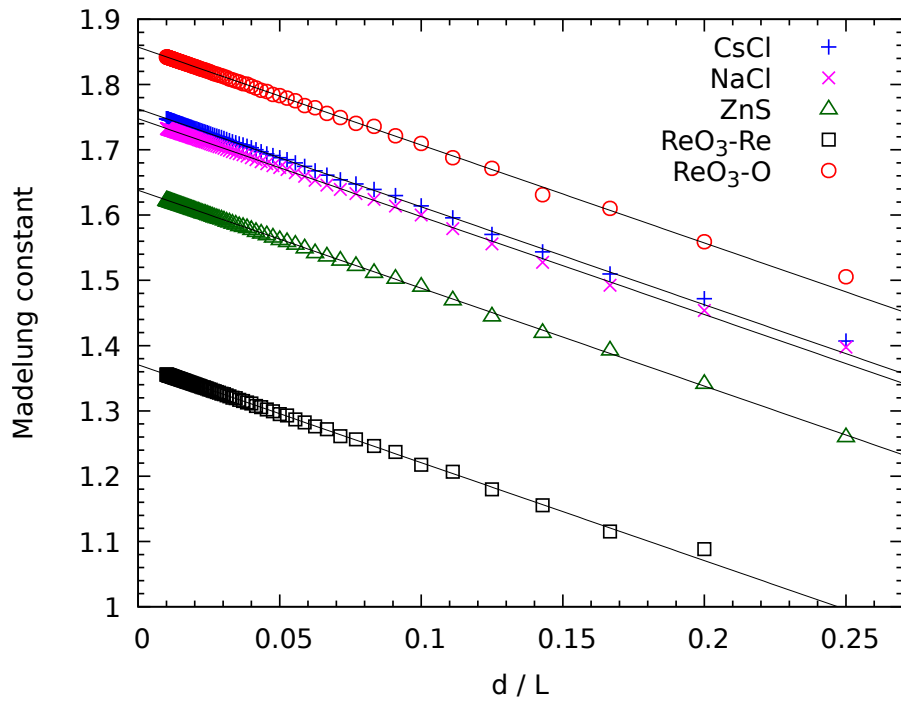


Figure 3: Ensemble averaged Madelung constant of a sphere of diameter L , for NaCl, CsCl, ZnS and ReO_3 structures with nearest neighbor distance d . The lines are $M_\alpha^\infty - 1.5d/L$, where M_α^∞ is the infinite crystal value.

is the mean square charge of the ions. We stress that Eq. (32) corresponds to the spherical average over all surface orientations. As we have made no assumption about the crystal structure, this result is universal, i.e. it holds for any crystal and amorphous structure. For binary systems, it simplifies to $U^S = \rho q^2/8$.

The ensemble averaged surface energy of Eq. (32) can be considerably larger than the surface energies found in real ionic crystals. For NaCl, for example, Eq. (32) gives 1.28 J/m², which is several times larger than the experimental values reported for the low index surfaces (100) and (110), which are 0.15–0.18 J/m² and 0.35–0.45 J/m², respectively [17]. The main reason for this discrepancy is that U^S is an average over all surface orientations, which includes all kinds of vicinal surfaces as well as highly unstable polar faces. Real crystals, however, are faceted, and only the most stable, low index surfaces are actually present in crystallites. Second, ionic and electronic relaxation and reconstruction, not considered here, make the surface energy decrease further, especially for stepped and polar terminations.

4.2 Relative stability of finite clusters

Despite the fact that Eq. (32) overestimates the surface energy of ionic crystals, the present findings, which are valid for all ionic systems, provide important insight into the size dependence of the Madelung energy. In particular, we can understand trends in the relative stability of different structures as a function of system size. From Eqs. (7,31) the ensemble averaged Madelung energy of a subvolume V with an average of $N = \rho V$ ions is given, to first order in $1/L$, by

$$U = -\frac{N}{2d} \sum_{\alpha} c_{\alpha} q_{\alpha}^2 \left(M_{\alpha}^{\infty} - \frac{3d}{2L} \right), \quad (34)$$

where $c_{\alpha} = N_{\alpha}/N$ is the concentration of α ions. Using Eq. (34) the ensemble averaged Madelung energy of finite clusters of different crystal structures can be compared. We write $d/L = \chi/N^{1/3}$, where χ is a geometrical factor that only depends on the crystal structure and the shape of the subvolume. In the following we consider binary structures, where $c_{+} = c_{-} = 1/2$, $q_{+} = -q_{-}$ and $M_{+} = M_{-}$. As the most simple example, we compare two ionic structures with the same nearest neighbor distance d , which is a reasonable assumption when cations and anions have about the same ionic radius. From Eq. (34) we then find the energy difference between the two clusters

$$\Delta U = -\frac{Nq^2}{2d} \left(\Delta M^{\infty} - \frac{3\Delta\chi}{2N^{1/3}} \right). \quad (35)$$

where $\Delta X = X_1 - X_2$ ($X = U, M^\infty, \chi$). We label the two structures such that $\Delta M^\infty > 0$, i.e. structure 1 is the stable phase in the bulk. If $\Delta\chi > 0$, then ΔU changes sign at the cluster size

$$N_0 = \left(\frac{3\Delta\chi}{2\Delta M^\infty} \right)^3. \quad (36)$$

Then, structure 1 is stable for $N > N_0$ and structure 2 for $N < N_0$. As an example, we compare CsCl (structure 1) and NaCl (structure 2). We have $M_1^\infty = 1.762675$ (CsCl), $M_2^\infty = 1.747565$ (NaCl) and so $\Delta M^\infty = 0.015110$. We consider spherical volumes. It is easy to see from simple geometrical relations that $\chi_1 = \sqrt{3}/2 \times (\pi/3)^{1/3}$ (CsCl) and $\chi_2 = (\pi/6)^{1/3}$ (NaCl), which gives $\Delta\chi = 0.073445$. From Eq. (36) we then obtain $N_0 = 388$. So the model predicts a phase transition from the NaCl structure to the CsCl structure when the cluster size exceeds about 400 atoms. The model may be applied to CsBr, CsCl and CsI, where the ionic radius of cation and anion is about the same (Cs=1.81Å, Cl=1.67Å, Br=1.82Å, I=2.06Å). In the bulk, these compounds crystallize in the CsCl structure. For small clusters, however, the NaCl structure has been observed in experiment [18, 19] and found to be more stable in first principles calculations [20, 21]. According to a recent experiment on neutral CsBr clusters, the transition from the NaCl to the CsCl structure occurs for a cluster size of about 160 atoms [19], in good agreement with our simple model.

5 Conclusions

In summary, we have developed a theory of ensemble averaged Madelung energies in finite volumes. The Madelung constants approach the thermodynamic limit in a universal way, independent of the structure, may it be crystalline or amorphous. A simple, general expression has been derived for the Madelung part of the termination averaged surface energy. The size dependence of the Madelung energies helps to understand the relative stability of different ionic structures as a function of system size, and provides a simple explanation for the phase transition from the rocksalt to the cesium chloride structure, which is observed in CsX clusters (X=Cl,Br,I).

Acknowledgments

I thank Jean-Marc Simon and Thijs Vlugt for stimulating discussions. This work was supported by JSPS KAKENHI Grant Number 19K05383.

References

- [1] P. P. Ewald, Die Berechnung optischer und elektrostatischer Gitterpotentiale, *Ann. Phys.* **369**, 253 (1921).
- [2] A. D. Baker and M. D. Baker, Madelung Constants of Nanoparticles and Nanosurfaces, *J. Phys. Chem. C* **113**, 14793 (2009).
- [3] R. M. Martin, *Electronic structure: basic theory and practical methods*, Cambridge University Press, New York, 2004.
- [4] D. Borwein, J. M. Borwein and K. F. Taylor, Convergence of lattice sums and Madelung constant, *J. Math. Phys.* **26**, 2999 (1985).
- [5] H. M. Evjen, On the Stability of Certain Heteropolar Crystals, *Phys. Rev.* **39**, 675 (1932).
- [6] E. I. Izgorodina, U. L. Bernard, P. M. Dean, J. M. Pringle and D. R. MacFarlane, The Madelung Constant of Organic Salts, *Cryst. Growth Des.* **9**, 4834 (2009).
- [7] D. Wolf, P. Keblinski, S. R. Phillpot and J. Eggebrecht, Exact method for the simulation of Coulombic systems by spherically truncated, pairwise r^{-1} summation, *J. Chem. Phys.* **110**, 8254 (1999).
- [8] W. A. Harrison, Simple calculation of Madelung constants, *Phys. Rev. B* **73**, 212103 (2006).
- [9] D. A. McQuarrie, *Statistical Mechanics*, Harper and Row, New York, 2000.
- [10] J. G. Kirkwood, and F. P. Buff, The statistical mechanical theory of solutions. I, *J. Chem. Phys.* **19**, 774 (1951).
- [11] P. Krüger, S. K. Schnell, D. Bedeaux, S. Kjelstrup, T. J. H. Vlugt and J.-M. Simon, KirkwoodBuff integrals for finite volumes *J. Phys. Chem. Lett.* **4**, 235 (2013).
- [12] N. Dawass, P. Krüger, S. K. Schnell, D. Bedeaux, S. Kjelstrup, J.-M. Simon and T. J. H. Vlugt, Finite-size effects of Kirkwood-Buff integrals from molecular simulations, *Mol. Sim.* **44**, 599 (2018).
- [13] P. Krüger and T. J. H. Vlugt, Size and shape dependence of finite-volume Kirkwood-Buff integrals, *Phys. Rev. E* **97**, 051301(R) (2018).

- [14] N. Dawass, P. Krüger, J.-M. Simon and T. J. H. Vlugt, Kirkwood-Buff integrals of finite system: shape effects, *Mol. Phys.* **116**, 1573 (2018)
- [15] A. Santos, Finite-size estimates of Kirkwood-Buff and similar integrals, *Phys. Rev. E* **98**, 063302 (2018).
- [16] A. Ben-Naim, *Molecular Theory of Solutions*, Oxford Univ. Press (2006).
- [17] P. W. Tasker, The surface energies, surface tensions and surface structure of the alkali halide crystals, *Phil. Mag. A* **39**, 119 (1979).
- [18] Y. J. Twu, C. W. S. Conover, Y. A. Yang, and L. A. Bloomfield, Alkali-halide cluster ions produced by laser vaporization of solids, *Phys. Rev. B* **42**, 5306 (1990).
- [19] L. Hautala, K. Jänkälä, T. Löytynoja, M.-H. Mikkilä, N. Prisle, M. Tchapyguine, and M. Huttula, Experimental observation of structural phase transition in CsBr clusters *Phys. Rev. B* **95**, 045402 (2017).
- [20] A. Aguado, A. Ayuela, J. M. Lopez, and J. A. Alonso, Ab initio calculations of structures and stabilities of $(\text{NaI})_n\text{Na}^+$ and $(\text{CsCl})_n\text{Cs}^+$ cluster ions, *Phys. Rev. B* **58**, 9972 (1998).
- [21] A. Aguado, Emergence of bulk CsCl structure in $(\text{CsCl})_n\text{Cs}^+$ cluster ions, *Phys. Rev. B* **62**, 13687 (2000).